



# Analysis of Stress-Deformation Behavior of Soil-Geosynthetic Composites in Plane Strain Condition

Jonathan T. H. Wu<sup>1</sup> · Chih-Yu Tung<sup>1</sup> ·  
Michael T. Adams<sup>2</sup> · Jennifer E. Nicks<sup>2</sup>

Accepted: 24 April 2018 / Published online: 9 May 2018  
© Springer Science+Business Media, LLC, part of Springer Nature 2018

**Abstract** A study was undertaken to investigate stress-deformation behavior of soil-geosynthetic composites (SGC) by finite element method of analysis. Five field-scale experiments conducted on *representative* SGC of different reinforcement stiffness/strength and reinforcement spacing were used to validate the analytical model. An elasto-plastic soil model, referred to as the hardening soil model, was selected to simulate behavior of compacted fill in the SGC experiments. Model parameters were determined from results of large-size triaxial compression tests by following a set of procedure without back-calculation or calibration. Measured external and internal displacements, including vertical strains, horizontal displacement profiles, and internal movement at selected points of all five SGC tests, were found to be in very good agreement with simulation results from the analytical model up to an applied pressure of 1000 to 2000 kPa. The validated model therefore serves as a reliable tool for investigation of stress-deformation behavior of soil-geosynthetic composites. This paper presents validation of the analytical model, analysis of stresses and deformation of SGC, and influence of factors such as reinforcement stiffness, reinforcement spacing,

---

✉ Jonathan T. H. Wu  
Jonathan.wu@ucdenver.edu

Chih-Yu Tung  
Blue780431@gamil.com

Michael T. Adams  
Mike.adams@dot.gov

Jennifer E. Nicks  
Jennifer.nicks@dot.gov

<sup>1</sup> Reinforced Soil Research Center, University of Colorado Denver, Denver, CO 80217, USA

<sup>2</sup> Turner-Fairbank Highway Research Center, Federal Highway Administration, 6300 Georgetown Pike, McLean, VA 22101, USA

soil stiffness and strength parameters on stress-deformation behavior of SGC. The study helps to gain improved understanding of stress-deformation behavior of soil-geosynthetic composites.

**Keywords** Soil-geosynthetic composite · GRS · Finite element analysis · Hardening soil model · Model parameter · Model validation · Parametric study

## Introduction

Modern technology of reinforced soil walls began in the 1960s, with inclusion of metallic strips in the compacted fill along with a wall face to acquire and maintain stability. Polymeric geosynthetics was later used as an alternative to metallic strips as reinforcement. These reinforced soil walls are designed by considering the inclusions as quasi-tieback tension members and commonly designed by using methods such as AASHTO Specifications [4], FHWA method [6], and NCMA method [11]. They are collectively referred to as Mechanically Stabilized Earth (MSE) walls. MSE walls with geosynthetics as reinforcement have sometimes been referred to as Geosynthetic Mechanically Stabilized Earth or simply GMSE.

Reinforcement spacing for GMSE walls is typically between 0.3 and 0.9 m. The relatively wide spacing stems from a fundamental design concept of a tieback system. In a tieback system, spacing of tieback plays a very minor role, as it is the total resisting force that matters. The significant beneficial effects of placing sheet reinforcement on small spacing, however, have gained increasing attention in recent years. The significant benefits of close reinforcement spacing were first realized in actual construction, and later validated by many field-scale experiments (1, 3, 7, 12, 19, 21). These experiments have confirmed that reinforcement spacing plays a far greater role than reinforcement strength in the capacity of a reinforced soil system. It has also been established that the behavior of reinforced soil with closely spaced geosynthetic reinforcement can be accurately characterized as a *soil-geosynthetic composite* [20, 21].

Geosynthetic Reinforced Soil (GRS) emerged as a new reinforced soil technology, as an alternative to GMSE, in the mid-2000s. GRS is designed by taking advantage of improved engineering characteristics of soil with closely spaced reinforcement [2]. The interaction between soil and closely spaced reinforcement forms a composite that relies on geosynthetics inclusion to reinforce the soil *internally*, and its stability does not rely on external support offered by the wall face. It should be noted that in the literature, the term GRS has sometimes been referred to all geosynthetic reinforced soil structures regardless of how it is designed.

Geosynthetic Reinforced Soil (GRS) bears strong resemblance to GMSE, in that both systems comprise three major components: compacted backfill, horizontally placed geosynthetic reinforcement, and facing (typically, dry-stacked concrete block facing). The main difference between the two systems lies in the fundamental design concepts. GRS considers the closely spaced geosynthetic sheets as reinforcing elements in a soil-geosynthetic composite (hence the term *reinforced* in GRS). GMSE, on the other hand, considers the reinforcement as quasi-tieback elements to help stabilize a pre-defined potential failure wedge (hence the term *stabilized* in GMSE). In GRS, wall

facing serves as a façade, as a protective element to prevent sloughing of soil, and as a construction aid; whereas in GMSE, facing is a load-carrying component, hence failure of a GMSE wall can be imminent if the facing fails. Due to the difference in design concept, reinforcement spacing of a GRS system usually ranges from 0.1 m (4 in.) in zones immediately beneath large concentrate vertical loads to 0.3 m (12 in.), with 0.2 m (8 in.) being typical, to acquire significant beneficial effects of soil-geosynthetic interaction, whereas the reinforcement spacing in a MSE system is usually much larger (0.3~0.9 m, or 12~36 in.), with 0.6 m (24 in.) being typical, to reduce construction time. Note that in the design of a tieback system, spacing of tieback presumably has little bearing on performance.

In current practice of earth retaining wall construction, GMSE enjoys much greater popularity than GRS. One reason for this is because GMSE is designed within the context of an externally stabilized wall system, of which the face is a structural component to retain soil and to resist earth pressure, much like, reinforced concrete gravity walls, cantilever reinforced concrete walls, anchored retaining walls, etc. Externally stabilized walls have been used for over a century. As with any paradigm change, many design engineers are either uncomfortable with or unaware of internally stabilized soil walls that rely on the reinforcing effect of tensile inclusion; as a result, many internally stabilized wall systems have incorporated some structural components of externally stabilized retaining walls to enhance stability, and many hybrid internally-externally stabilized GMSE walls have been built.

A majority of current design methods adopt the tieback design concept for these walls and have indirectly encouraged the use of wide reinforcement spacing. The result is a failure rate that is much too high to be considered a sound system. The National Concrete Masonry Association has estimated a 2 to 8% failure rate nationally for GMSE walls. Berg [5] and Valentine [17] have estimated that the failure rate of GMSE walls in the USA is as high as 5%. Koerner and Koerner [10] reported a database of 141 failed GMSE Walls, of which 107 were actual collapse, and 34 were unserviceable due to excessive deformation. Holtz [9] indicates that bulging of wall face is an issue for GMSE walls. In a recent survey, many state DOTs list excessive bulging and deformation as a top concern for GMSE walls [8].

This paper reports a study undertaken to investigate stress-deformation behavior of soil-geosynthetic composites for GRS in plane strain condition. The analytical model was critically validated by comparing simulated displacements with measured external and internal displacements of one unreinforced and four *soil-geosynthetic composite* (SGC) tests in plane strain condition. These tests vary in reinforcement stiffness/strength, reinforcement spacing, and confinement condition. Using the validated analytical model, stress distribution within the soil-geosynthetic composites when subject to increasing vertical pressures was examined to gain insight into the stresses in soil-geosynthetic composites. A parametric study was also conducted to examine the influence of reinforcement spacing, reinforcement stiffness, soil stiffness and strength on stress-deformation behavior of soil-geosynthetic composites. This paper describes validation of the analytical model, presents the stress distribution in soil-geosynthetic composites under different vertical pressures, and discusses findings of the parametric study.

## Representative Soil-Geosynthetic Composites and SGC Tests

Due to the presence of geosynthetic inclusion, a reinforced soil mass is inherently non-uniform. To investigate stress-deformation behavior of a non-uniform mass, the dimensions of a representative test specimen are of critical importance. A series of finite element analyses were initially performed to determine the dimensions of a test specimen needed in order to adequately characterize soil-geosynthetic composite behavior on 0.2-m reinforcement spacing in plane strain conditions [13, 20]. With a length/height ratio of 0.7, specimen heights of 7.0, 2.0, 1.0, and 0.5 m under a plane strain condition were examined numerically. Considering a soil-geosynthetic composite of 7.0 m high by 4.9 m wide with reinforcement spacing of 0.2 m as a prototype composite mass, it was found that specimen heights  $H = 1.0$  m and  $H = 0.5$  m are too small to provide adequate representation, but that a 2.0-m high by 1.4-m long specimen would provide sufficiently accurate (within  $\pm 10\%$  deviations) representation for the composite. For purposes of comparison, a parallel series of finite element analyses were also performed for soil specimens without any reinforcement. Specimen height as small as 0.5 m was found to yield nearly the same stress-strain-volume change relationships as those of a uniform soil mass of  $H = 7.0$  m when no reinforcement was present. This suggests that while a small specimen is adequate for investigating behavior of a uniform soil mass, a much larger specimen is needed for investigating reinforced soil behavior.

Table 1 lists the conditions of the SGC tests. The test specimens were 2.0 m in height, 1.4 m in length, and 1.2 m in width (in the plane strain direction). Since these tests replicate the reinforcement spacing used in actual construction in the field, the term “field-scale” is used for description. All five experiments were performed in a plane strain condition (see Fig. 1). The backfill material used in the tests was A-1-a crushed diabase material, a well graded gravelly soil (GW) with largest particle size of 33 mm, and was compacted to 98% per ASTM D698. Relevant properties of the backfill are as follows: specific gravity of soil solids = 3.0, percentage of fines = 14.6%, maximum dry unit weight = 24.1 kN/m<sup>3</sup>, and optimum water content = 5.2%. Five large-size (diameter = 152 mm, height = 305 mm) consolidated drained triaxial tests were performed at confining pressures ranging from 34 to 760 kPa (5 to 110 lb/in<sup>2</sup>).

**Table 1** Test conditions of one unreinforced test (Test 1) and four SGC tests (Tests 2, 3, 4, and 5)

Test designation	Geosynthetic reinforcement	Confining pressure	Wide-width strength of reinforcement	Reinforcement spacing, $s_v$
Test 1	None	34 kPa	None	No reinforcement
Test 2	Woven polypropylene geotextile	34 kPa	$T_j = 70$ kN/m	$s_v = 0.2$ m
Test 3	Double-sheet of Test 2	34 kPa	$T_j = 140$ kN/m	$s_v = 0.4$ m
Test 4	Same as Test 2	34 kPa	$T_j = 70$ kN/m	$s_v = 0.4$ m
Test 5	Same as Test 2	0 kPa (unconfined)	$T_j = 70$ kN/m	$s_v = 0.2$ m

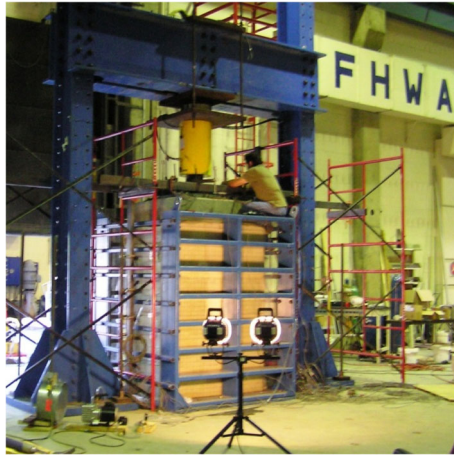


**Fig. 1** Field-scale plane strain Soil-Geosynthetic Composite (SGC) test

The stress-strain-volume change relationship is shown in Fig. 2. The Mohr-Coulomb strength parameters are as follows:  $c$  (cohesion) = 70 kPa,  $\phi$  (angle of internal friction) =  $48^\circ$  for confining pressures of 35, 105, and 210 kPa. The reinforcement used in the tests was a woven polypropylene geotextile with a wide width tensile strength, per ASTM D4595, of 70 kN/m, in both warp and fill directions. The reinforcement of Test 3 was formed by gluing two sheets of the geotextile together. Wide-width tensile tests performed on the glued specimen show that the stiffness and strength were approximately twice those of a single sheet geotextile. Detailed information of the SGC tests has been presented by Pham [13] and Wu et al. [21].

## Finite Element Simulation of Soil-Geosynthetic Composites

Finite element (FE) method of analysis was employed to simulate the field-scale SGC experiments described in section “[Representative Soil-Geosynthetic Composites and SGC Tests](#)”. The analysis was conducted by using the finite element code Plaxis 8.2. In the analysis, geosynthetic reinforcement was simulated by a linear elastic model, of which the material parameters are shown in Table 2. The soil-reinforcement contact surface was assumed to be fully bonded. Use of interface elements along soil-reinforcement contact surface in the analysis was also performed. The interface friction angle of  $(2/3) \tan \phi = 36^\circ$  and interface adhesion of  $(2/3) c = 46.7$  kPa were assumed. The results were nearly identical with or without interface elements, which confirmed that the assumption of fully bonded soil-reinforcement interface was valid.

The hardening soil model was selected for simulation of the behavior of the fill material in the SGC tests. It is a second-order hyperbolic elasto-plastic hardening model involving friction hardening to express the plastic shear strain in deviatoric loading and cap hardening to express the plastic volumetric strain in primary compression. The model was selected because it is capable of simulating many important soil characteristics, such as stress-dependency, non-linearity, stress-path dependency, and dilatancy. The soil parameters of the hardening soil model determined from drained triaxial

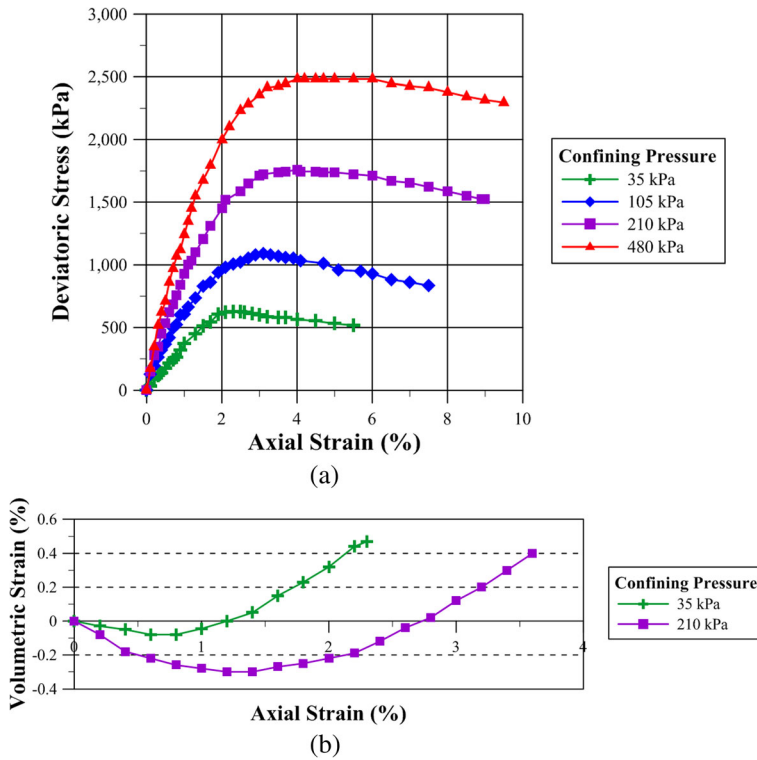


Fig. 2 a Stress-strain behavior and b volume change behavior of the diabase in triaxial compression tests

compression tests at relevant confining pressures are included in Table 2. These parameters are average values at confining pressures of 35, 105, and 210 kPa (or 5, 15, and 30 psi), the range of confining pressure relevant to the SGC experiments. Note that there was no calibration or back-calculations involved in parameter selection. A

Table 2 Material parameters for the finite element analysis

Material	Material model	Parameters and values
Soil (a diabase)	Hardening model [15]	dry unit weight, $\gamma_d = 24 \text{ kN/m}^3$ ; moist unit weight, $\gamma_m = 25 \text{ kN/m}^3$ ; cohesion, $c = 70 \text{ kPa}$ ; angle of internal friction, $\phi = 48^\circ$ ; angle of dilation, $\psi = 17^\circ$ ; soil moduli (as defined in [14]), $E_{30}^{ref} = 63,400 \text{ kPa}$ , $E_{ur}^{ref} = 126,800 \text{ kPa}$ , $E_{oed}^{ref} = 54,800 \text{ kPa}$ ; Poisson's ratio $\nu = 0.2$ ; failure ratio, $R_f = 0.9$ ; stress-dependency power parameter, $m = 0.5$
Reinforcement (a woven geotextile)	Linear elastic model	Test 1 no reinforcement Test 2 axial stiffness, $EA = 700 \text{ kN/m}$ Test 3 axial stiffness, $EA = 1400 \text{ kN/m}$ Test 4 axial stiffness, $EA = 700 \text{ kN/m}$ Test 5 axial stiffness, $EA = 700 \text{ kN/m}$

detailed description of the material parameters, including how they were obtained, has been given by Wu and Tung [22]. The following describes validation of the analytical model by comparisons with measured vertical strains (section “[Model Validation by Vertical Strains](#)”), lateral displacement profiles (section “[Model Validation by Lateral Displacement Profiles](#)”), and internal displacements at selected points (section “[Model Validation by Internal Displacements at Selected Points](#)”) of the SGC tests.

### **Model Validation by Vertical Strains**

Comparisons of simulated and measured applied vertical pressure vs. vertical (axial) strain relationships of the five field-scale SGC tests are shown in Fig. 3. For Tests 3 and 4, the agreement between simulated and measured behavior was excellent up to 1000 kPa; for Test 2, the agreement was excellent up to 2000 kPa. Past these pressures, measured deformation became increasingly larger than simulated values. It was suspected that this could be a result of large deformation under high applied pressures not being accounted for in the analyses. The analyses were repeated using updated Lagrangian analysis in which the finite element mesh was continuously updated during the calculation. The analysis results differed insignificantly from those of small strain analyses. It is reasoned that the discrepancy at high applied pressure is mainly because the hardening soil model does not account for any time-dependent deformation, whereas the measured value does include significant time-dependent deformation at higher applied pressures. Regardless, a 1000 kPa vertical pressure is five times the typical design pressure for typical GRS abutments which indicates that the model is capable of providing a good simulation of vertical deformation, especially at service level conditions.

### **Model Validation by Lateral Displacement Profiles**

Comparisons of simulated and measured lateral displacement profiles under various applied vertical pressures for the five field-scale SGC tests are shown in Fig. 4. It is seen that there is a good overall agreement between the modeled and measured lateral displacement profiles under all levels of applied vertical pressure for all five experiments.

### **Model Validation by Internal Displacements at Selected Points**

Internal movements at selected points of the soil-geosynthetic composites in the SGC tests were monitored using grid lines marked on the lubricated latex membrane system. Previous study of the lubrication technique indicates that the friction angle with the plaxiglass side wall is less than one (1.0) degree [18]. Details of the system have been previously described by Pham [13] and Wu et al. [21]. Comparisons of simulated and measured internal displacements at five selected points in Test 2 (reinforcement strength  $T_f$ , reinforcement spacing  $s_v$ ) and Test 3 (reinforcement strength  $2*T_f$ , reinforcement spacing  $2*s_v$ ) are shown in Fig. 5. The simulated and measured path of the internal movement at the selected points illustrate that the agreement is excellent at every selected point under all pressure levels.



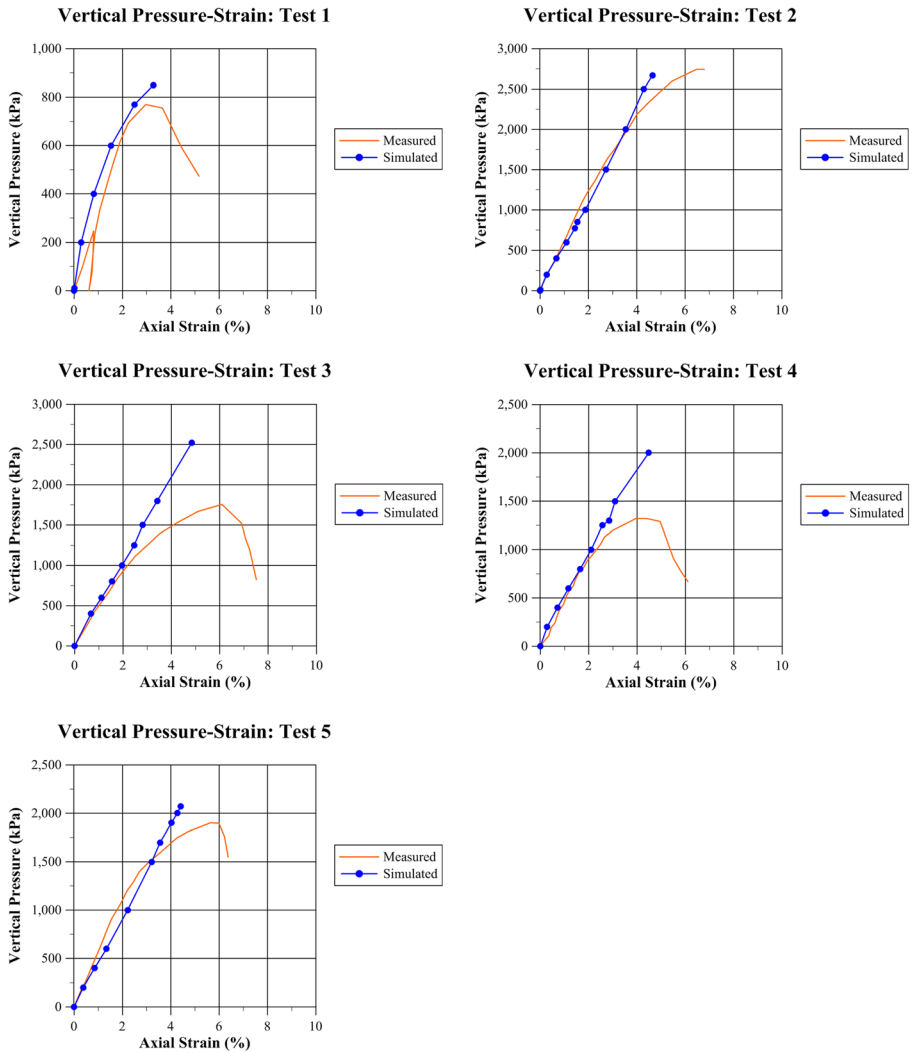


**Fig. 3** Comparisons of simulated and measured applied vertical pressure vs. vertical (axial) strain relationships of the five SGC tests

### Analysis of Stress Distribution in Soil-Geosynthetic Composites

A distinct advantage with finite element analysis of earth structures is the ability to analyze stresses in the soil mass that are otherwise very difficult to measure accurately during physical experiments. Of course, this advantage can only be realized if the stresses obtained by finite element analysis method are reliable, i.e., if the analysis results agree with “all” measured *displacement fields* of the entire earth structure. In this study, the comparison of the simulated and measured external and internal displacements agreed well, hence provides an opportunity to examine stresses within a SGC with good confidence.



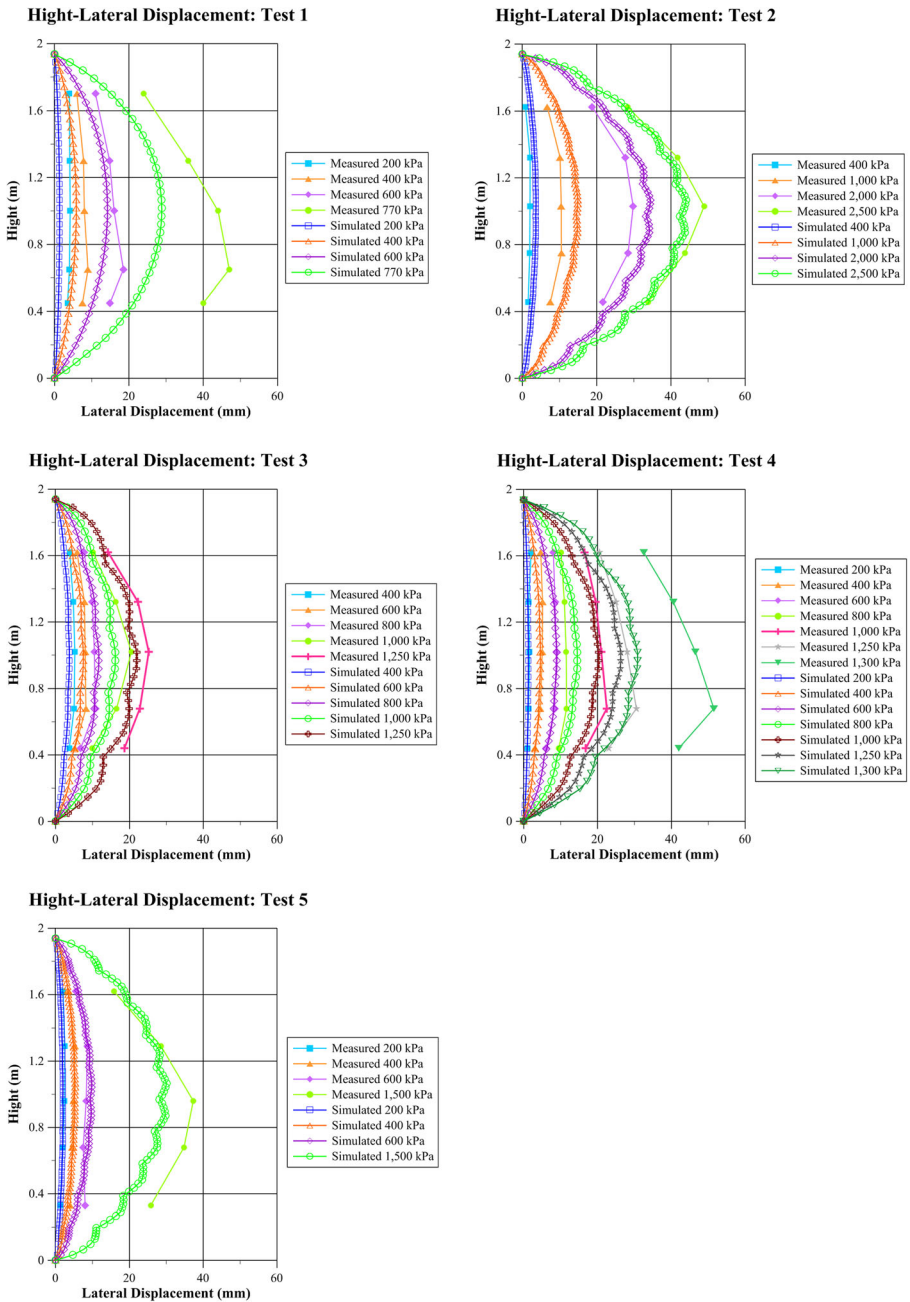


**Fig. 4** Comparisons of simulated and measure lateral displacement profiles under various applied vertical pressures for the five SGC tests

Figure 6a, b shows distributions of vertical stress and lateral stress, respectively, within the unreinforced soil mass (Test 1) and reinforced soil mass (Test 2) (with  $T_f =$

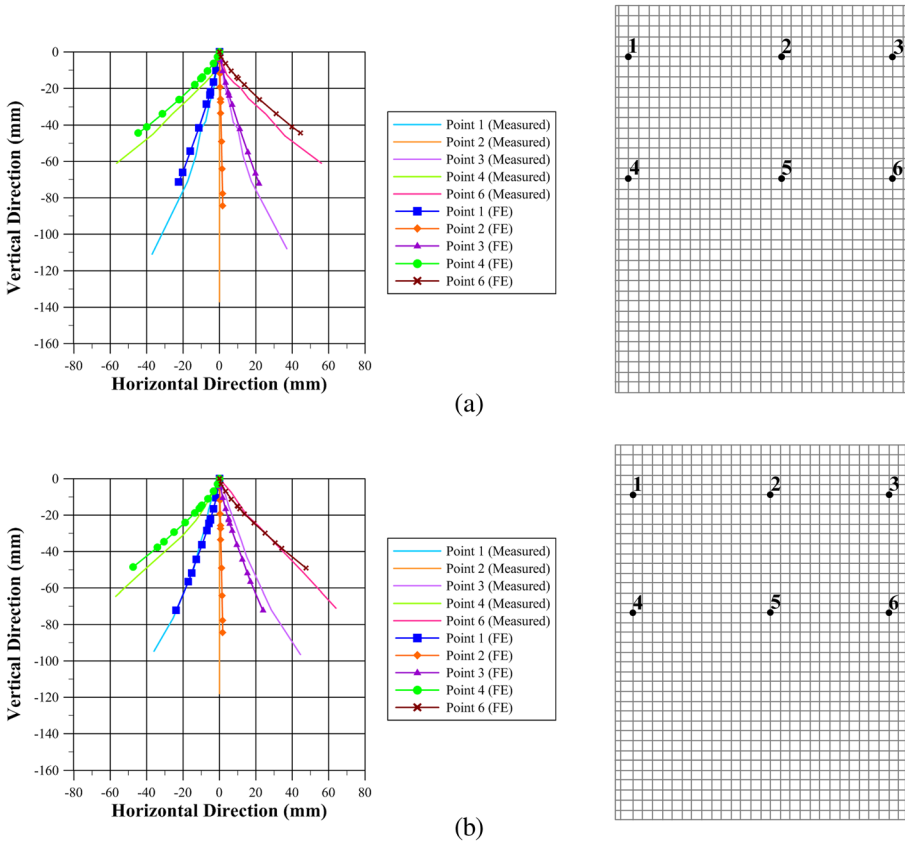


**Fig. 5** Comparisons of simulated and measure internal displacements at five selected points when subject to increasing vertical pressure for **a** Tests 2 and **b** Test 3 [note: point 5 is not shown in this figure to avoid confusion]

70 kN/m and  $s_v = 0.2$  m) under applied vertical pressure of 10 kPa. Note that 10 kPa vertical pressure corresponds to a typical design load for non-load-bearing walls subjected to the normal traffic condition. Note also that the reinforcement strength and reinforcement spacing of Test 2 is typical for GRS abutments and walls. The results indicate the vertical stresses within the unreinforced soil mass and the reinforced soil mass are essentially the same. The lateral stresses of the two soil masses, however, are evidently different, with the lateral stress in the reinforced soil mass being higher, especially near the reinforcement layers. The higher lateral stress within the reinforced soil mass is due to higher restraint of lateral deformation resulting from bonding at the soil-reinforcement interface. Greater confining pressure leads to higher stiffness and strength of a soil; greater compressive lateral stress resulting from geosynthetic inclusion leads to a stiffer and stronger SGC. The benefit of increased lateral stress has long been identified as a reinforcing mechanism of reinforced soil (e.g., [16, 23]). The stress distributions seen in Fig. 6 also confirm that.

Figure 7a, b shows distributions of vertical stress and lateral stress, respectively, within the unreinforced soil mass (Test 1) and reinforced soil mass (Test 2) (with  $T_f = 70$  kN/m and  $s_v = 0.2$  m) under applied vertical pressure of 200 kPa. Note that 200 kPa

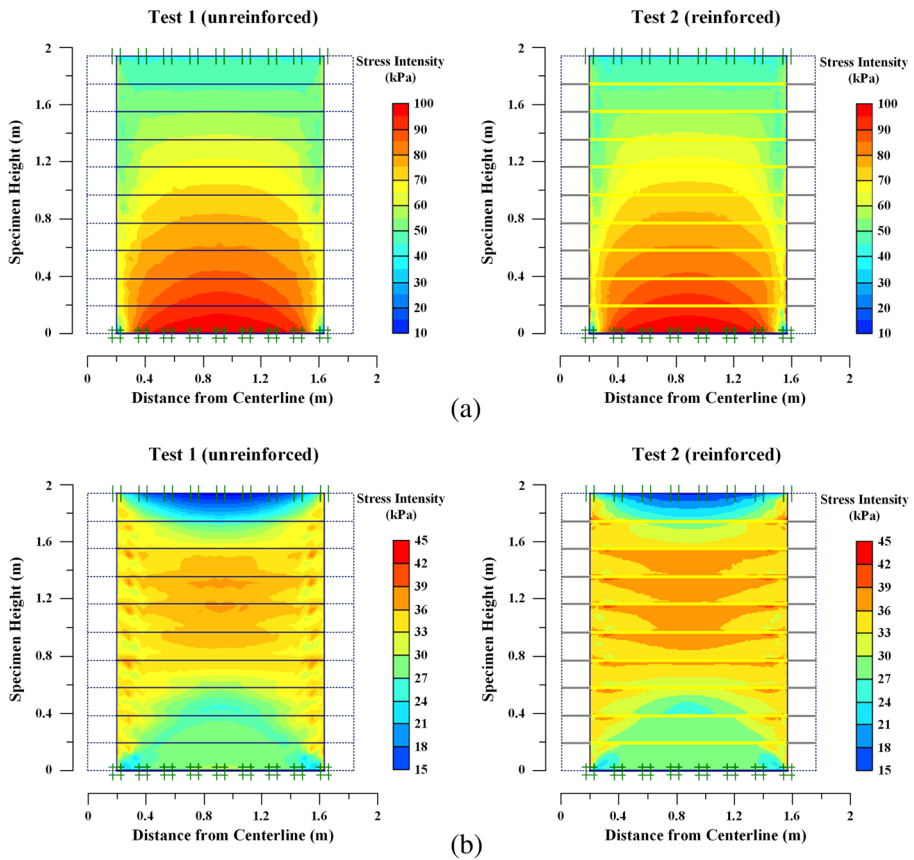


**Fig. 6** Distributions of **a** vertical stresses and **b** lateral stress within the soil mass in Test 1 (unreinforced) and Test 2 (reinforced), under applied vertical pressure of 10 kPa

is a typical design load commonly used for GRS bridge abutments [6]. It is seen that the vertical stresses in the unreinforced and reinforced soil masses are nearly the same, with the latter being slightly lower than the former. The lateral stress in the reinforced soil mass is again higher than in the unreinforced soil mass, especially near the vertical face of the reinforced soil mass. The higher lateral stress in the reinforced soil mass is a result of higher restraint of lateral deformation due to soil-reinforcement friction.

Figure 8a, b shows distributions of vertical stress and lateral stress, respectively, in the unreinforced soil mass (Test 1) and reinforced soil mass (Test 2) (with  $T_f = 70$  kN/m and  $s_v = 0.2$  m) under applied vertical pressure of 600 kPa. The vertical pressure corresponds to a surcharge that is three times a typical design load for GRS bridge abutments. It is seen that the vertical stresses in the reinforced soil mass are significantly lower than that in the unreinforced soil mass. This indicates that the closely spaced reinforcement layers generate positive arching in the reinforced soil mass under high surcharge (600 kPa in this case). The lateral stress distribution within reinforced soil mass is again seen to be higher than that in the unreinforced soil mass. The increase in lateral stress is seen to be more

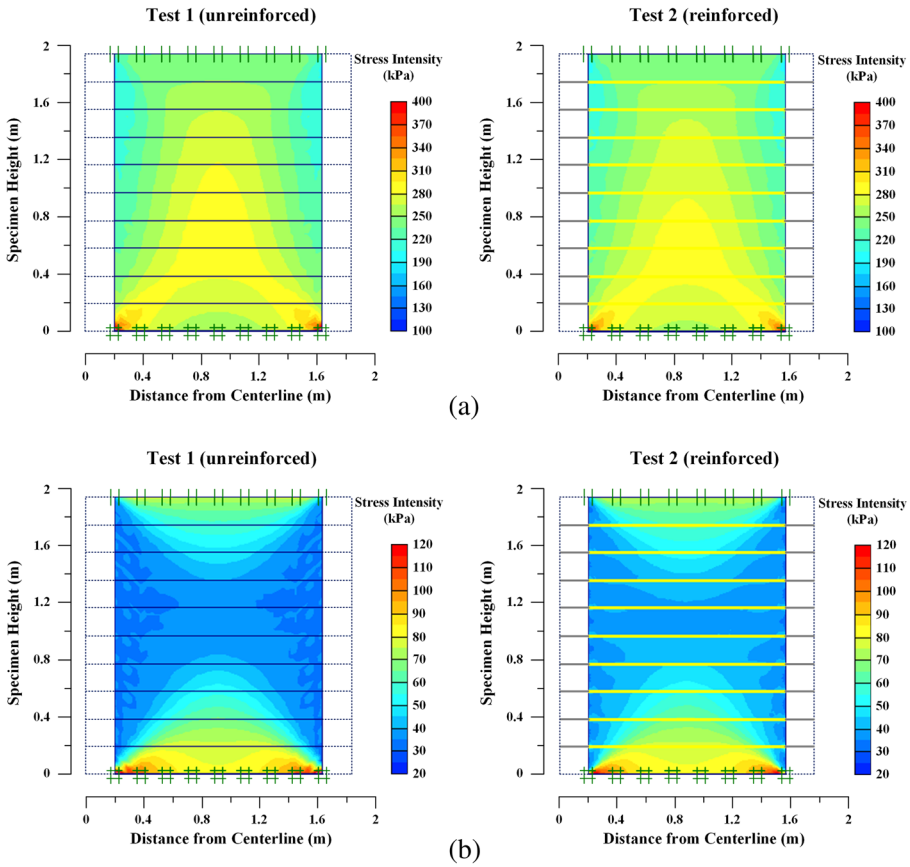


**Fig. 7** Distributions of **a** vertical stress es and **b** lateral stress within the soil mass of in Test 1 (unreinforced) and Test 2 (reinforced), under applied vertical pressure of 200 kPa

pronounced under 600 kPa vertical pressure than under 200 kPa. The positive arching (in terms of vertical stress) in conjunction with increased lateral stress results in lower shear stress levels, hence a composite that is less likely to reach a failure condition.

### Parametric Study

A parametric study was conducted to examine the influence of six factors, including reinforcement axial stiffness ( $EA$ ), reinforcement spacing ( $s_v$ ), cohesion ( $c$ ), friction angle ( $\phi$ ), dilation angle ( $\psi$ ), and soil stiffness parameters ( $E_{50}$ ,  $E_{ur}$  &  $E_{oed}$ ) on stress-deformation behavior of soil-geosynthetic composites. The parametric study was performed by selecting a baseline soil-geosynthetic composite with a common set of material and geometric parameters given in Table 3. When studying the effect of a certain factor, all parameters are kept the same as in the baseline case except for the particular parameters under investigation.

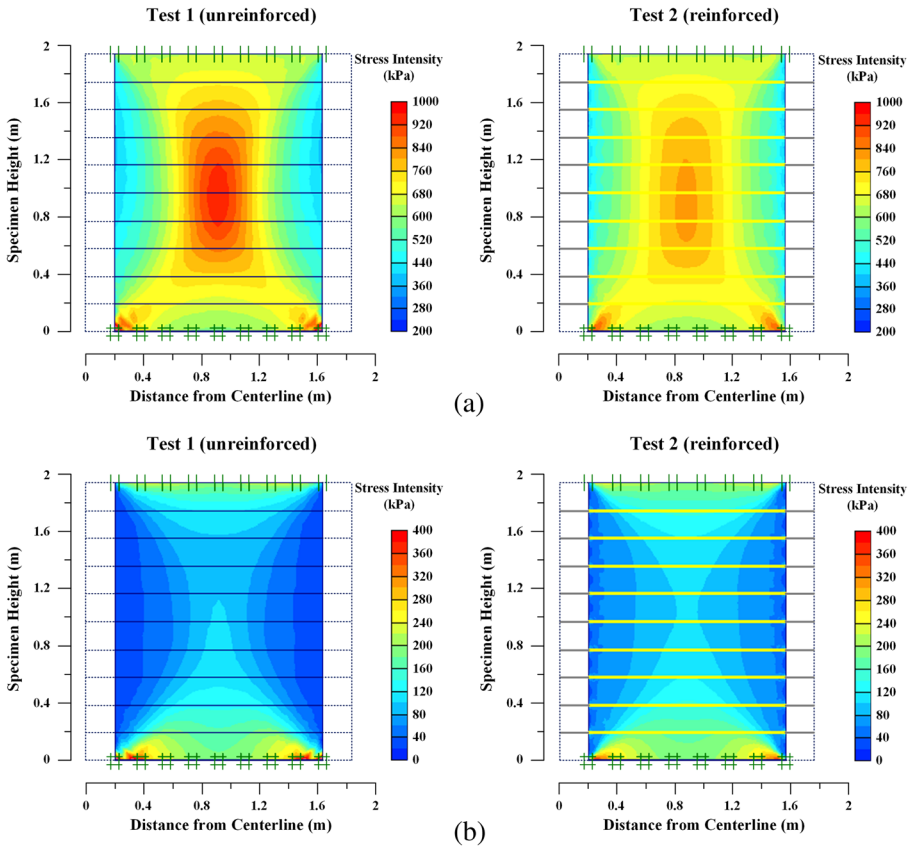


**Fig. 8** Distributions of **a** vertical stresses and **b** lateral stress within the soil mass in Test 1 (unreinforced) and Test 2 (reinforced), under applied vertical pressure of 600 kPa

In addition to the baseline case, a total of 14 cases were analyzed. The 14 cases are divided into six groups, each group is to examine a particular factor, as shown in

**Table 3** Parameters for the baseline case of parametric study

Material	Material model	Parameters and values
Soil (Crushed Diabase-A-1-a)	Hardening model [15]	dry unit weight, $\gamma_d = 24 \text{ kN/m}^3$ ; moist unit weight, $\gamma_m = 25 \text{ kN/m}^3$ ; cohesion, $c = 70 \text{ kPa}$ ; angle of internal friction, $\phi = 48^\circ$ ; angle of dilation, $\psi = 19^\circ$ ; soil moduli (as defined in [14]): $E_{50}^{ref} = 63,400 \text{ kPa}$ , $E_{ur}^{ref} = 126,800 \text{ kPa}$ , $E_{oed}^{ref} = 54,800 \text{ kPa}$ ; Poisson's ratio $\nu = 0.2$ ; failure ratio, $R_f = 0.9$ ; stress-dependency power parameter, $m = 0.5$
Reinforcement (woven polypropylene geotextile)	Linear elastic model	Axial stiffness, $EA = 700 \text{ kN/m}$ ; ultimate strength, $T_{ult} = 70 \text{ kN/m}$ ; reinforcement spacing, $s_v = 0.2 \text{ m}$

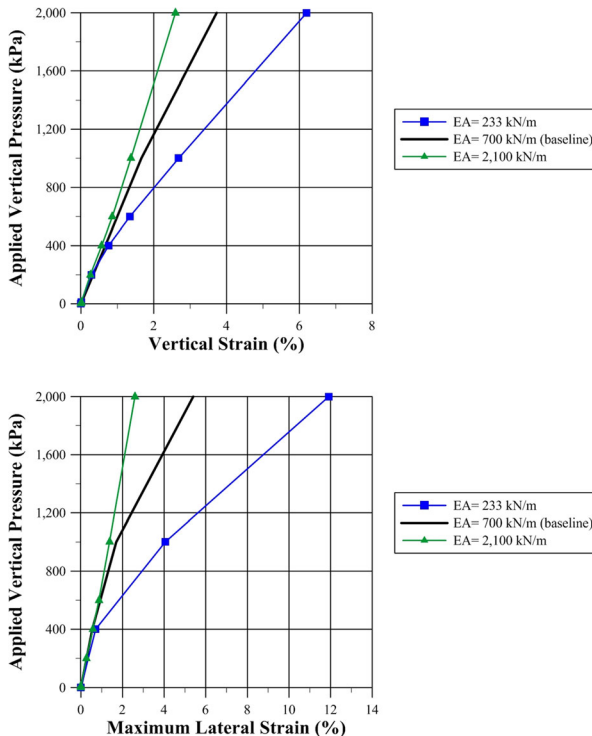
**Table 4** Groups of parametric study

Group	Parameter	Parameter values <sup>a</sup>	Results
A	$EA$ (reinforcement stiffness)	$EA = 233 \text{ kN/m}; 700 \text{ kN/m}; 2100 \text{ kN/m}$	Fig. 9
B	$s_v$ (reinforcement spacing)	$s_v = 0.1 \text{ m}; 0.2 \text{ m}; 0.4 \text{ m}$	Fig. 10
C	$c$ (soil strength parameter)	$c = 0 \text{ kPa}; 70 \text{ kPa}; 170 \text{ kPa}$	Fig. 11
D	$\phi$ (soil strength parameter)	$\phi = 38^\circ; 43^\circ; 48^\circ; 53^\circ$	Fig. 12
E	$\psi$ (soil dilation angle)	$\psi = 0^\circ; 10^\circ; 19^\circ; 30^\circ$	Fig. 13
F	$E_{50}, E_{ur},$ and $E_{oed}$ (soil stiffness)	$1/3 * E_{baseline}; E_{baseline}; 3 * E_{baseline}$	Fig. 14

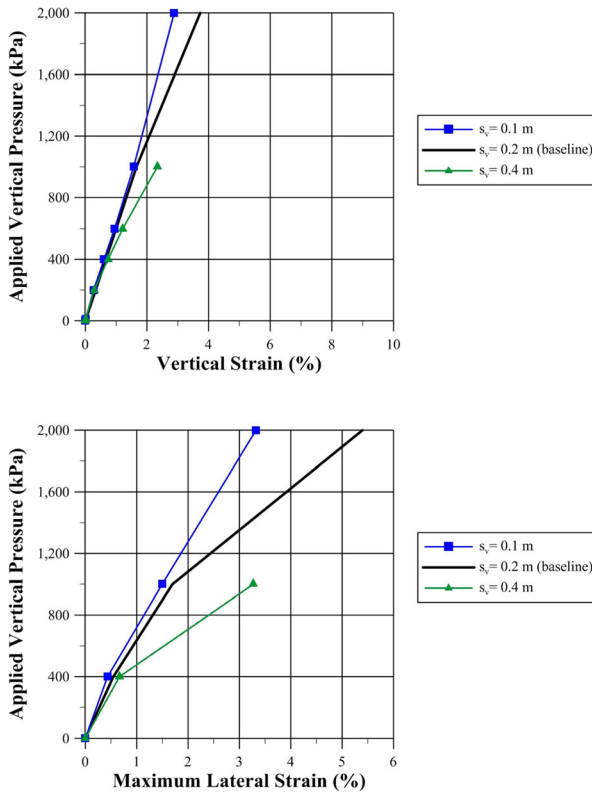
<sup>a</sup> All other parameters were kept the same as in the baseline case except for the specific parameter under investigation

Table 4. Note that, when appropriate, the parameters are varied by a ratio of 1/3 and 3 of the value in the baseline case. Table 4 also shows the figure number in which results of each group are presented.

Figure 9 shows the influence of reinforcement axial stiffness, represented by the product of Young’s modulus ( $E$ ) and cross-sectional area ( $A$ ), on vertical pressure vs. vertical strain and vertical pressure vs. maximum lateral strain relationships. As expected, higher  $EA$  value of reinforcement results in a stiffer SGC. It is interesting to note that the influence of reinforcement axial stiffness ( $EA$ ) is negligible up to



**Fig. 9** Influence of reinforcement axial stiffness ( $EA$ ) on load-deformation behavior of SGCC



**Fig. 10** Influence of reinforcement spacing ( $s_v$ ) on load-deformation behavior of SGC

vertical pressure of about 400 kPa. However, as the vertical pressure exceeds 400 kPa, the effect of EA becomes more significant. Note also that the effect of EA is noticeably greater as it changes from  $1/3 \cdot EA$  (233 kN/m) to  $EA$  (700 kN/m) than from  $EA$  (700 kN/m) to  $3 \cdot EA$  (2100 kN/m).

The influence of vertical reinforcement spacing ( $s_v$ ) on vertical pressure vs. vertical strain and vertical pressure vs. maximum lateral strain relationships is shown in Fig. 10. The anticipated response was that the stiffness of SGC would increase with closer reinforcement spacing. However, Fig. 10 indicates that when vertical pressure is less than 400 kPa, the influence of reinforcement spacing on both vertical and lateral deformation is negligible for  $s_v$  between 0.1 and 0.4 m. The influence of varying reinforcement spacing from 0.2 to 0.4 m on deformation becomes significant when vertical pressure exceeds 400 kPa. For  $s_v$  between 0.1 and 0.2 m, the deformation is essentially unaffected when vertical pressure is between 400 and 1000 kPa. For reinforcement spacing of 0.4 m, the analysis indicates that failure will occur at vertical pressure of 1000 kPa. The effect of reinforcement spacing as noted above needs to be viewed with caution because it was tacitly assumed that the stiffness of the soil in the soil mass is unaffected by the reinforcement spacing. The presence of the reinforcement is known to restrain lateral deformation of the soil due to soil-reinforcement friction. As a result, the *compaction-induced stress* (i.e., residual lateral stress due to the loading/unloading process of a compaction load) will be more pronounced in a reinforced soil



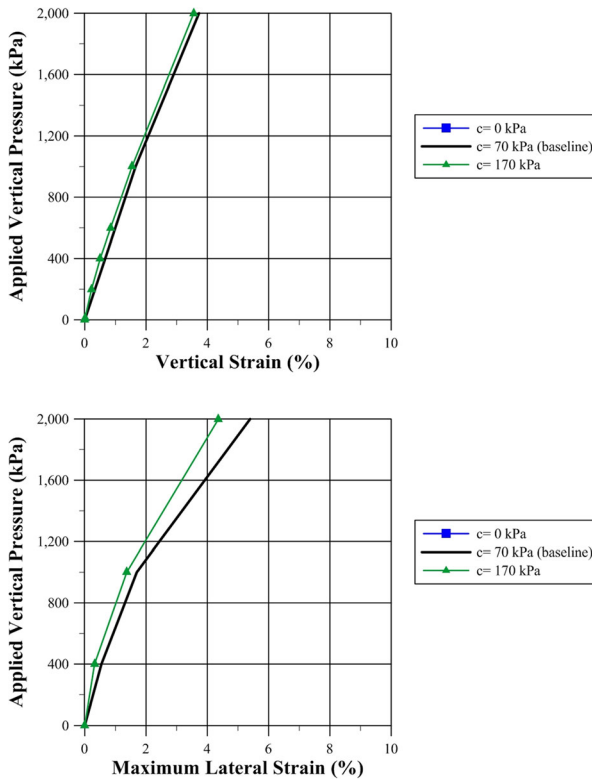


**Fig. 11** Influence of cohesion ( $c$ ) on load-deformation behavior of SGC [note: for  $c = 0$ , the soil mass failed as the 6th soil lift was placed]

mass with smaller reinforcement spacing. The higher the compaction-induced stress, the higher the lateral stress, hence higher soil stiffness. This effect is not accounted for in the analysis shown in Fig. 10.

The influence of Mohr-Coulomb strength parameter  $c$  (cohesion) on vertical pressure vs. vertical strain and vertical pressure vs. maximum lateral strain relationships of the SGC is shown in Fig. 11. As illustrated, the influence of cohesion on vertical pressure vs. vertical strain is very small. The effect is slightly more pronounced for vertical pressure vs. maximum lateral strain relationship, although the effect is still quite small. The analysis also indicates that the SGC will fail during construction (when the 6th soil lift was placed) for the SGC with zero cohesion. The results of  $c = 0$  are therefore not included in Fig. 11.

Figure 12 shows the vertical pressure vs. vertical strain and vertical pressure vs. maximum lateral strain relationships of the SGC as Mohr-Coulomb strength parameter  $\phi$  (angle of internal friction) varied from  $38^\circ$  to  $53^\circ$ ; the baseline friction angle was  $48^\circ$ . For vertical pressure leading to 400 kPa, the influence of  $\phi$  on vertical pressure vs. vertical strain and vs. maximum lateral strain relationships is negligible; however, when vertical pressure exceeds 400 kPa, the effect of  $\phi$  becomes significant for  $\phi = 38^\circ$  and  $43^\circ$ ; for higher  $\phi$ -values ( $\phi = 48^\circ$  and  $53^\circ$ ), the threshold pressure is at about 1000 kPa for significant difference in deformation. The analysis also indicates that reinforcement near the mid-height will rupture at vertical pressure of about 1500 kPa for  $\phi = 38^\circ$ .

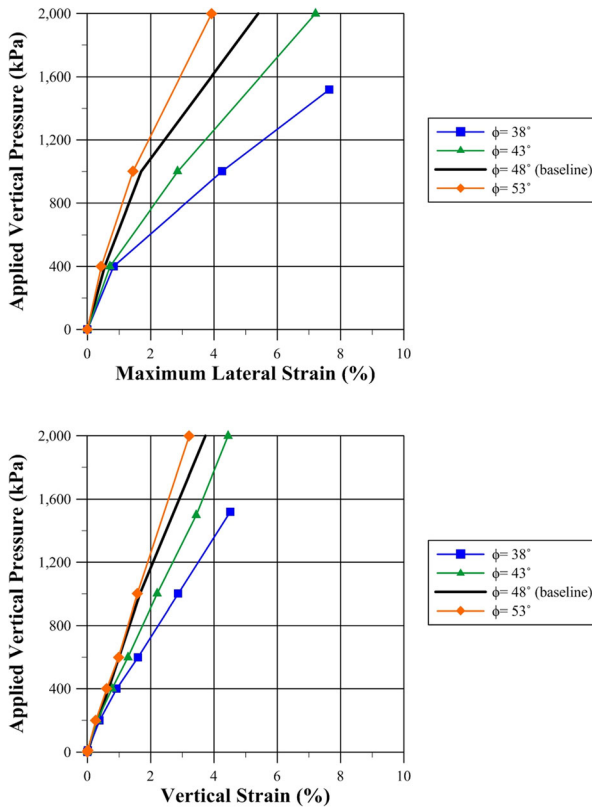


**Fig. 12** Influence of angle of friction ( $\phi$ ) on load-deformation behavior of SGC [note: for  $\phi = 38^\circ$ , reinforcement layer #5 ruptured at applied vertical pressure of 1500 kPa]

The influence of angle of dilation ( $\psi$ ) of the fill material on load-deformation behavior of SGC as  $\psi$  varies from 0 to  $30^\circ$  is shown in Fig. 13. The influence of  $\psi$  on vertical pressure vs. vertical strain relationship is very small up to a threshold pressure of 500 kPa. Above 500 kPa, the influence of  $\psi$  is modest, except for  $\psi \leq 10^\circ$  for which the threshold vertical pressure is about 1000 kPa. Above the threshold pressure, the vertical stiffness generally increases with  $\psi$ -value. The influence of  $\psi$  on vertical pressure vs. maximum lateral strain relationship is also negligible up to vertical pressure of 500 kPa; above 500 kPa, the lateral stiffness generally increases with increasing vertical pressure. The analysis also indicates that for  $\psi = 0^\circ$ , reinforcement near the mid-height will rupture under an applied vertical pressure of 1600 kPa.

Soil stiffness, as characterized by parameters  $E_{50}$ ,  $E_{ur}$ , and  $E_{oed}$ , had by far the greatest influence on vertical and lateral load-deformation behavior of SGC. Among all factors investigated, soil stiffness is the only one that has appreciable effect on stress-deformation relationships of SGC under vertical pressure of 200 kPa, a typical design pressure for GRS bridge abutments. This confirms that soil stiffness is the most important material parameter that influences the stress-deformation behavior of SGC. As expected, the higher the soil stiffness, the stronger the SGC (see Fig. 14). Note that the relationship between soil stiffness and SGC stiffness is not linear, in that the

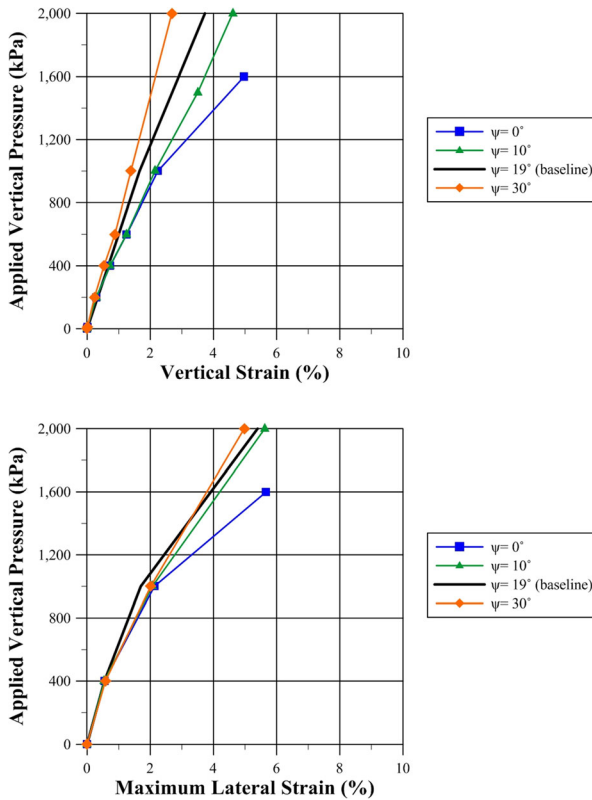


**Fig. 13** Influence of angle of dilation ( $\psi$ ) on load-deformation behavior of SGC [note: for  $\psi = 0^\circ$ , layer #5 ruptured at applied vertical pressure of 1600 kPa]

difference in SGC stiffness between soil stiffness  $1/3 * E$  and  $E$  is significantly greater than that between  $E$  and  $3 * E$ .

### Concluding Remarks

Geosynthetic Reinforced Soil (GRS) differs from MSE with Geosynthetics as reinforcement (GMSE) in the design concept. For the former, closely spaced geosynthetic layers interact with surrounding soil to form soil-geosynthetic composites, whereas for the latter geosynthetic layers are considered tension tieback elements to stabilize potential failure soil wedges. More attention is now being given to GRS due to concerns over performance issues and an alarmingly high failure rate of GMSE.

This study was undertaken to investigate stress-deformation behavior of soil-geosynthetic composites (SGC) by the finite element method of analysis. The finite element model used in this study accurately simulated “all” measured external (i.e., on exposed surfaces) and internal displacements of five sets of soil-geosynthetic composite tests under increasing applied vertical pressure. The five tests vary in reinforcement stiffness/strength, reinforcement spacing, and confinement condition. Successful simulation of all the tests suggests that the model is very reliable and can be used with

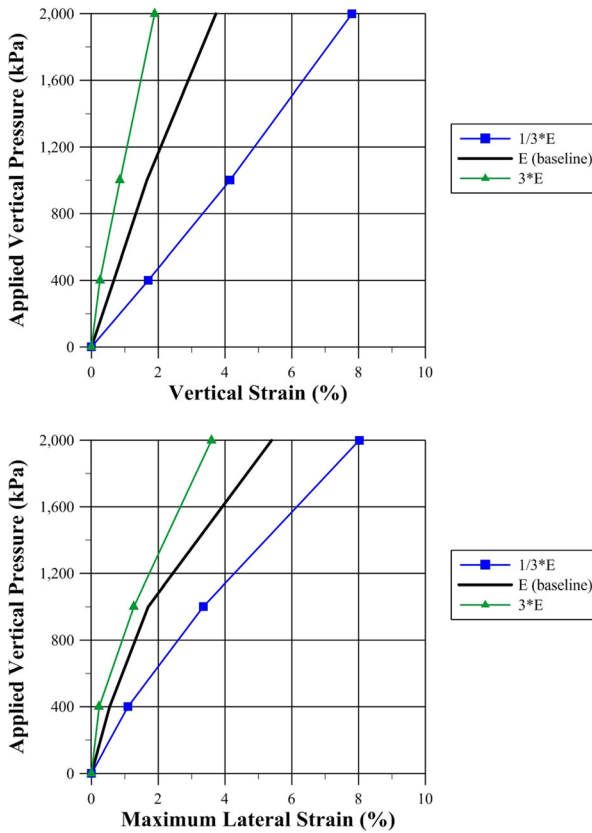


**Fig. 14** Influence of soil stiffness ( $E_{50}$ ,  $E_{ur}$  and  $E_{oed}$ ) on load-deformation behavior of SGC

confidence to analyze stress-deformation behavior of the soil-geosynthetic composites under the given set of conditions.

The study indicates that, under typical design loads (i.e., applied vertical pressure not more than 200 kPa), the vertical stresses in closely spaced reinforced soil and in unreinforced soil are practically the same. The lateral stresses, however, are significantly higher in reinforced soil than in unreinforced soil. For applied vertical pressure much greater than typical design loads, the vertical stresses in reinforced soil are significantly lower than those in unreinforced soil. In other words, positive arching occurred in the reinforced soil mass and is especially pronounced under high applied vertical pressure. The arching behavior tends to produce lower shear stress levels, hence less likely to reach a failure condition compared to unreinforced soils.

The parametric study conducted by using the validated analytical model allows examination of the influence of reinforcement stiffness, reinforcement spacing, soil strength, and soil stiffness on stress-deformation behavior of soil-geosynthetic composites. It suggests that as long as the fill is sufficiently stiff (as in the baseline case given in Table 3), reinforcement axial stiffness, reinforcement spacing, soil strength parameters all have negligible to very small influence on stress-deformation behavior of the soil-geosynthetic composites under 400 kPa applied vertical pressure. Soil stiffness

is clearly the most important among all the factors. This confirms a rule of thumb: *When it comes to improved performance of GRS, there is no substitute for high soil stiffness.* Note that soil stiffness is affected by fill material type, fill placement condition, compaction equipment, and compaction lift.

## References

1. Adams, M.T., Lillis, C.P., Wu, J.T.H., and Ketchart, K.: Vegas Mini Pier Experiment and Postulate of Zero Volume Change. Proceedings, Seventh International Conference on Geosynthetics, pp. 389–394. Nice (2002)
2. Adams, M.T., Nicks, J.E., Stabile, T., Wu, J.T.H., Schlatter, W., Hartmann, J.: Geosynthetic Reinforced Soil Integrated Bridge System Interim Implementation Guide, Report No. FHWA-HRT-11-026. Federal Highway Administration, McLean (2011)
3. Adams, M.T., Schlatter, W., and Stabile, T.: Geosynthetic-Reinforced Soil Integrated Abutments at the Bowman Road Bridge in Defiance County, Ohio. Proceedings, Geo-Denver 2007, ASCE, Denver (2007)
4. American Association of State Highway and Transportation Officials (AASHTO): LRFD Bridge Design Specifications, 7th Edition. (2014)
5. Berg, R.R.: Fill Walls - Recent Advances and Future Trends. Proceedings, 2010 Earth Retention Conference, pp. 1–19. American Society of Civil Engineers, Bellevue (2010)
6. Berg, R.R. Christopher, B.R., Samtani, N.C.: Design of Mechanically Stabilized Earth Walls and Reinforced Soil Slopes, Design & Construction Guidelines. Report No. FHWA-NHI-00-043, pp. 394. Federal Highway Administration, McLean (2009)
7. Elton, D.J., Patawaran, M.A.B.: Mechanically Stabilized Earth (MSE) Reinforcement Tensile Strength from Tests of Geotextile Reinforced Soil. Technical Report, Alabama Highway Research Center, Auburn University (2005)
8. Gerber, T.M.: Assessing the Long-Term Performance of Mechanically Stabilized Earth Walls. *NCHRP Synthesis 437*, National Cooperative Highway Research Program, Transportation Research Board, Washington D.C. (2012)
9. Holtz, R.D.: Reinforced Soil Technology: from Experimental to the Familiar. Terzaghi Lecture, GeoFlorida, Palm Beach. (2010)
10. Koerner, R.M. and Koerner, G.R.: A Data Base and Analysis of 141 Failed Geosynthetic Reinforced Mechanically Stabilized Earth (MSE) Walls. Proceedings, 26<sup>th</sup> Central Pennsylvania Geotechnical Conference (2012)
11. National Concrete Masonry Association (NCMA): *Design Manual for Segmental Retaining Walls*, 3rd Edition (Collin, ed.), p. 281 (2009)
12. Nicks, J.E., Adams, M.T., Ooi, P.S.K.: Geosynthetic reinforced soil I performance testing – Axial load deformation relationships. Report No. FHWA-HRT-13-066, Federal Highway Administration, McLean (2013)
13. Pham, T. Q.: Investigating Composite behavior of Geosynthetic-Reinforced Soil (GRS) Mass. Ph.D. Dissertation, University of Colorado Denver (2009)
14. Plaxis B.V.: Plaxis 2D - Version 8 Manual. Balkema, Rotterdam (2002)
15. Schanz, T., Vermeer, P.A., Bonnier, P.G.: Formulation and Verification of the Hardening Soil Model. In: Brinkgreve, R.B.J. (ed.) Beyond 2000 in Computational Geotechnics, pp. 281–290. Balkema, Rotterdam, The Netherlands (1999)
16. Schlosser, F. and Long, N.C.: La Terre ArmeedansL'Echageur de Sete. *Revue Generale des Rates et des Aerodromes*, No. 480 (1972)
17. Valentine, R.J.: An Assessment of the Factors that Contribute to the Poor Performance of geosynthetic-Reinforced Earth Retaining Walls. Proceedings, Design and Practice of Geosynthetic-Reinforced Soil Structures (Ling et al., Editors), Bologna, Italy, pp. 318–327 (2013)
18. Wu, J.T.H.: Construction and Instrumentation of the Denver Walls, pp. 21–30. International Symposium on Geosynthetic-Reinforced Soil Retaining Walls, Balkema, Rotterdam (1992)
19. Wu, J.T.H.: "Revising the AASHTO Guidelines for Design and Construction of GRS Walls." Report No. CDOT-DTD-R-2001-6, Colorado Department of Transportation (2001)
20. Wu, J.T.H., Pham, T.Q.: Load carrying capacity and required reinforcement strength of closely spaced soil-Geosynthetic composites. *J. Geotech. Geoenviron., ASCE*. 139(9), 1468–1476 (2013)

21. Wu, J.T.H., Pham, T.Q., Adams, M.T.: Composite Behavior of Geosynthetic Reinforced Soil Mass.” Report No. FHWA-HRT-10-077, p. 211. Turner-Fairbank Highway Research Center, FHWA, McLean (2013)
22. Wu, J.T.H., Tung, S.: Two-Dimensional GRS Model: Model Description and Validation. Task Order 11, GRS Modeling, Report submitted to Federal Highway Administration (2015)
23. Yang, Z.: Strength and Deformation Characteristics of Reinforced Sand. Ph.D. Dissertation, University of California at Los Angeles (1972)